Proceedings of the 8th IEEE Mediterranean Conference
on Control and Automation (MED 2000)
Rio, Patras, GREECE 17-19 July, 2000

CORRIDOR FOLLOWING BY MOBILE ROBOTS EQUIPPED WITH PANORAMIC CAMERAS

DIMITRIS P. TSAKIRIS[†], **ANTONIS A. ARGYROS** [†]

[†]Institute of Computer Science, FORTH, P.O. Box 1385, GR–711 10, Heraklion, Crete, Greece, {tsakiris, argyros}@ics.forth.gr

Abstract. The present work considers corridor–following maneuvers for nonholonomic mobile robots, guided by sensory data acquired by panoramic cameras. The panoramic vision system provides information from an environment with textured walls to the motion control system, which drives the robot along a corridor. Panoramic cameras have a 360° visual field, a capability that the proposed control methods exploit. In our sensor–based control scheme, optical flow information from several distinct viewing directions in the entire field of view of the panoramic camera is used directly in the control loop, without the need for state reconstruction. The interest of this lies in the fact that the optical flow information is not sufficient to reconstruct the state of the system, it is however sufficient for the proposed control law to accomplish the desired task. Driving the robot along a corridor amounts to the asymptotic stabilization of a subsystem of the robot's kinematics and the proposed control schemes are shown to achieve this goal.

Key Words. Nonholonomic mobile robots, path following, sensor–based control, panoramic cameras.

1. INTRODUCTION

Corridor–following maneuvers for mobile robots with nonholonomic constraints are considered, which are guided by sensory data acquired by panoramic cameras. A vision system with a 360° visual field provides information from an environment with textured walls to the motion control system, which drives the robot along a corridor.

The main advantage of panoramic cameras is that they are not constrained by a limited field of view, like classical camera setups. Robotic tasks requiring movement in one direction while observing environmental features in a different one, can then be more easily implemented.

In navigation tasks of mobile robots, the main alternatives to panoramic cameras are moving cameras (e.g. mounted on pan–and–tilt platforms or hand–eye systems) and multiple–camera systems mounted on the robot. In the case of moving cameras, their precise positioning, especially when the mobile robot is also moving, may be a challenging control problem. Looking in a direction outside from the current field of view of the camera, requires repositioning the sensor, which involves a delay that may be unacceptable when the environment also changes. This problem becomes more severe when the direction where the camera needs to look next is not known a–priori; time-consuming exploratory actions are then necessary. In the case of multiple–camera systems, the lack of a common nodal point of the cameras and the elaborate calibration required, complicate their use. The duplication of optical and electronic components increases the cost of the system. Moreover, the system lacks flexibility in observing an arbitrary direction of interest. In contrast to the above, panoramic cameras offer the capability of extracting information simultaneously from all desired directions of their visual field. Neither moving parts, nor elaborate control mechanisms or expensive hardware is required to achieve this capability.

A panoramic image generated by a camera with a paravoloid mirror (like the ones that we consider in this work) can be thought of as a collection of images acquired by ordinary perspective cameras that share a common nodal point. This property simplifies significantly

the derivation of the necessary information [8], [13]. The advantages of these sensors with respect to the solution of the 3D motion estimation problem, are also well known [3].

Biological systems are known to exploit wide field–of–view images in controlling their motion. The velocity of the perceived relative motion between the moving biological observer and its environment (optical flow), inferred from such image sequences, can be used to control the motion of the observer. Bees, for example, have laterally–pointing eyes, which amounts to a wide f.o.v., and use optical flow from such images to infer distance flown and control their flight [2], [12].

Sensor–based control strategies for robotic systems are well developed for manipulator arms; visual servoing, for instance, which consists in the direct use of visual information in a system's control loop [5], provides relatively simple and robust solutions to various positioning and tracking tasks. Their extension to the case of mobile robots is of significant importance for practical applications (e.g. in automating car driving maneuvers). However, it becomes complicated by the presence of nonholonomic kinematic constraints in the motion of the mobile base, necessitating the use of nonlinear control analysis and design tools [14].

Vision–based path–following tasks, similar to ours, are considered in [9], [1] and [4]. In [9], a two–camera system is considered, which is mounted on a mobile robot, with the cameras facing opposite lateral directions. The disparity between the average optical flow from the cameras is used in a PID loop controlling the angular velocity of the robot, while this moves at constant speed along a wall. In [1], optical flow information from a particular arrangement of three perspective cameras guides a path–following task. In [4], a landmark–based method for the reconstruction of the pose of a mobile robot from panoramic images is presented. The reconstructed pose is, then, fed into the nonlinear state–feedback path–following scheme developed in [10], [11]. From the image understanding viewpoint, this reconstruction is a difficult and error–prone procedure, which we attempt to bypass in our scheme. These works do not attempt, in general, a stability analysis of the resulting control scheme.

The task that we attempt to accomplish amounts to the asymptotic stabilization of a subsystem of the robot's kinematics. Optical flow information from several distinct viewing directions is used. After being derotated, it provides an estimate of the scaled difference of inverse depths in these directions. Our sensor–based control scheme employs this estimate directly in the control loop, without reconstructing the state of the system. This is very much in the spirit of visual servoing schemes. The resulting control law is shown, using Lyapunov's indirect method, to possess the necessary asymptotic stability properties, in the cases that the heading speed of the mobile robot remains strictly positive or negative over the entire duration of the task and in the case that it varies periodically.

2. MODELING

2.1. Mobile Robot Modeling

We consider a mobile robot of the unicycle type moving on a planar surface inside a corridor with straight parallel textured walls. We suppose that a panoramic camera is mounted on the robot (fig. 1).

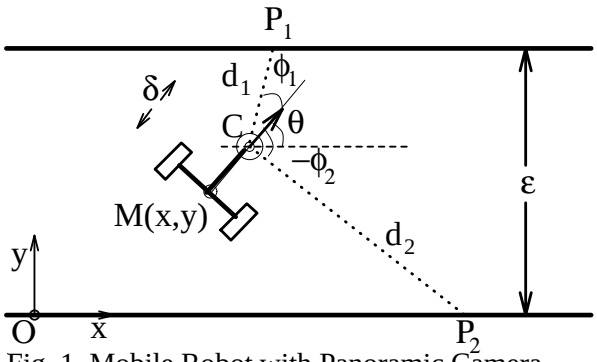

Fig. 1. Mobile Robot with Panoramic Camera

Consider an inertial coordinate system $\{F_O\}$ centered at a point O of the plane and aligned with one of the walls, a moving coordinate system $\{F_M\}$ attached to the middle M of the robot's wheel axis and another moving one $\{F_C\}$ attached to the nodal point C of the camera. Let (x, y) be the position of the point M and θ be the orientation of the mobile robot with respect to the coordinate system $\{F_O\}$. Let $\delta \geq 0$ be the distance of the point C from M and $\epsilon > 0$ the width of the corridor.

We suppose that the wheels of the mobile platform roll without slipping on the plane supporting the system. This induces a nonholonomic constraint on the motion of the mobile robot, due to the fact that the instantaneous velocity lateral to the heading direction of the mobile platform has to be zero. From this, we get the usual unicycle kinematic model for the mobile platform

$$\dot{x} = v\cos\theta\ ,\quad \dot{y} = v\sin\theta\ ,\quad \dot{\theta} = \omega\ , \tag{1}$$

where $v \stackrel{\text{def}}{=} \dot{x}\cos\theta + \dot{y}\sin\theta$ is the heading speed and ω is the angular velocity of the unicycle.

2.2. Panoramic Camera Modeling

Consider a pinhole camera and a camera-centered coordinate system $CXYZ$ positioned at its optical center C, with the CZ axis coinciding with the optical axis. Assume that the camera is moving rigidly with respect to its 3D static environment, with translational velocity (U, V, W) and rotational velocity (α, β, γ), both expressed with respect to its coordinate system. Under perspective projection, the relation between the 2D velocity $(u^x,\ u^y)$ of an image point p with image coordinates (x, y) and the 3D velocity of the corresponding 3D point

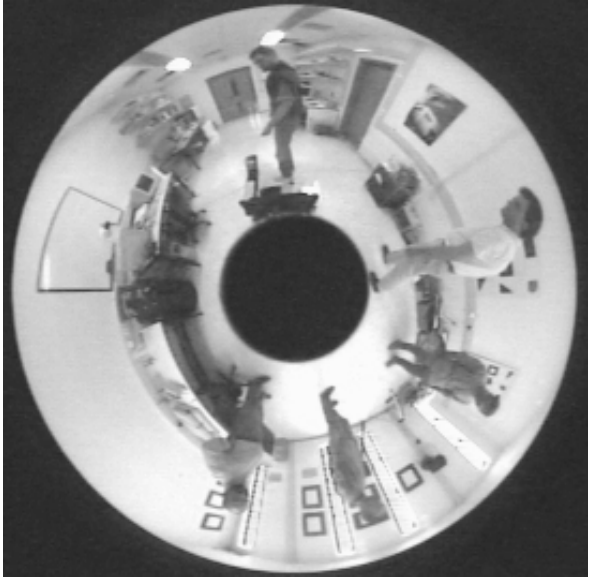

(a) Original Panoramic Image

(b) Corresponding Unfolded Cylindrical Image

Fig. 2. Panoramic Image

P with coordinates (X, Y, Z) is given by the optical flow equations [6]: $u^x = \frac{-Uf+xW}{Z} + \alpha\frac{xy}{f} - \beta\left(\frac{x^2}{f} + f\right) + \gamma y$, $u^y = \frac{-Vf+yW}{Z} + \alpha\left(\frac{y^2}{f} + f\right) - \beta\frac{xy}{f} - \gamma x$. Consider a mobile robot of the type described above, with a panoramic camera mounted on it, so that the symmetry axis of the paravoloid mirror coincides with the robot's axis of rotation (in the notation of fig. 1, this corresponds to $\delta = 0$.)

The panoramic image can be "unfolded" giving rise to a cylindrical image (fig. 2). Different columns of the resulting cylindrical image correspond to different viewing directions in the range $[0,\ 2\pi]$. We suppose that the heading direction of the robot is the one recorded on the cylindrical image column that corresponds to $\phi = \pi/2$ (fig. 2.b).

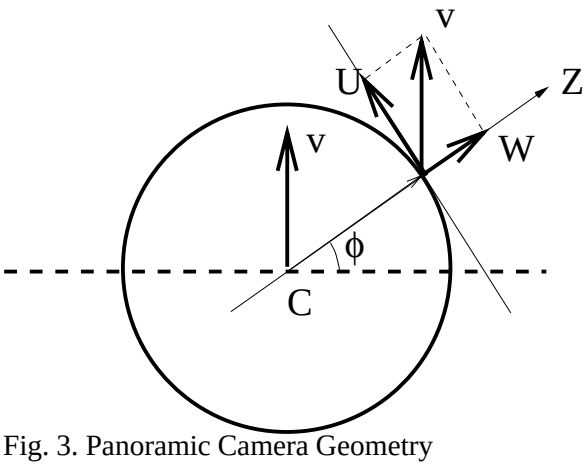

Fig. 3. Panoramic Camera Geometry

The resulting cylindrical images can be approximated by a number of perspective images that have no overlapping visual fields and which are tangent to the cylindrical surface. For these "virtual" perspective images, we may employ the optical flow equations to analyze the flow generated due to the robot's motion. More specifically, consider the column of the cylindrical image which corresponds to the viewing direction ϕ. Suppose that the part of the 3D scene projected on this column lies in depth d. The heading speed v of the robot results in two components of translational velocity in the image coordinate system: $W = v\sin\phi$ and $U = v\cos\phi$ (see fig. 3). Since we consider a robot that moves on a planar surface, the vertical component V of the camera's translational velocity becomes zero. Regarding the rotational velocity, only β is non–zero. By taking into account the above considerations, as well as the fact that $x \approx 0$ in the local coordinate systems of all "virtual" perspective cameras, the optical flow equations become:

$$u^x = -\frac{v\cos\phi f}{d} - \beta f\ , \quad u^y = \frac{y\ v\sin\phi}{d}\ . \qquad (2)$$

In the heading direction of the robot ($\phi = \pi/2$), the horizontal component of the optical flow u^x_h is equal to $-\beta f$, i.e. it depends only on the rotational component of the robot's motion.

Suppose now that we measure ([6]) the horizontal component of the optical flow $u^x_{\phi_1}$ and $u^x_{\phi_2}$ in two different directions ϕ_1 and ϕ_2, respectively, with corresponding depths d_1 and d_2. Define the quantities $\mathcal{L}_1 \stackrel{\text{def}}{=} u^x_{\phi_1} + u^x_{\phi_2} - 2\ u^x_h$ and $\mathcal{L}_2 \stackrel{\text{def}}{=} u^x_{\phi_1} - u^x_{\phi_2}$. It can be easily verified that $\mathcal{L}_1 = -vf(\frac{\cos\phi_1}{d_1} + \frac{\cos\phi_2}{d_2})$ and $\mathcal{L}_2 = -vf(\frac{\cos\phi_1}{d_1} - \frac{\cos\phi_2}{d_2})$. The depths d_1 and d_2 can, then, be specified from $\mathcal{L}_1$ and $\mathcal{L}_2$, which are measured directly from visual data, provided that the heading speed v of the robot is known or can be estimated.

Notice that in the case that the directions ϕ_1 and ϕ_2 are arranged symmetrically about the heading direction of the robot (when $\phi_1 = \frac{\pi}{2} + \phi$, $\phi_2 = \frac{\pi}{2} - \phi$, thus $\cos\phi_1 = -\cos\phi_2 = -\sin\phi$), the quantity $\mathcal{L}_1$ permits the estimation of the scaled difference of inverse depths, since $\mathcal{L}_1 = v\ f\sin\phi\ (\frac{1}{d_1} - \frac{1}{d_2})$.

Consider the rays d_1 and d_2 in the forward directions ϕ and $-\phi$ and the rays d_3 and d_4 in the backwards directions $-(\pi - \phi)$ and $\pi - \phi$, with respect to the heading direction of the robot (fig. 1). We suppose that d_1 and d_4 intersect the left wall, while d_2 and d_3 intersect the right wall of the corridor. The magnitudes of the rays (depths) are related to the parameters of the system and to the state of the robot as follows:

$$\begin{aligned} d_1 &= \frac{\epsilon - y - \delta\sin\theta}{\sin(\theta+\phi)}\ , \quad d_2 = -\frac{y + \delta\sin\theta}{\sin(\theta-\phi)}\ , \\ d_3 &= \frac{y + \delta\sin\theta}{\sin(\theta+\phi)}\ , \qquad d_4 = -\frac{\epsilon - y - \delta\sin\theta}{\sin(\theta-\phi)}\ . \end{aligned} \qquad (3)$$

We suppose that $y \in (0,\ \epsilon)$ and $\theta \in (-\phi,\ \phi)$, with $0 < \phi < \frac{\pi}{2}$. Thus, $\sin(\theta+\phi) \neq 0$ and $\sin(\theta-\phi) \neq 0$.

We saw that the scaled differences of inverse depths

$$\begin{aligned}\mathcal{L}_1^{1,2} &= u_1^x + u_2^x - 2u_h^x = vf\sin\phi\left(\frac{1}{d_1} - \frac{1}{d_2}\right),\\ \mathcal{L}_1^{3,4} &= u_3^x + u_4^x - 2u_h^x = vf\sin\phi\left(\frac{1}{d_4} - \frac{1}{d_3}\right)\end{aligned} \tag{4}$$

can be directly extracted from the panoramic camera data by calculating the optical flow at a total of five distinct directions. It is of interest to consider whether they suffice for the corridor following task, even though they are not sufficient for a full reconstruction of the state (y, θ).

3. MOTION CONTROL

3.1. The Task: Corridor Following

The task of following a straight–line corridor consists in using the angular velocity of the system to drive the lateral distance of the robot from the walls, as well as its orientation, to desired values. This amounts to asymptotically stabilizing the state (y, θ) of the subsystem

$$\dot{y} = v\sin\theta\ ,\quad \dot{\theta} = \omega \tag{5}$$

of the unicycle kinematics 1 to $(y_\star,\ \theta_\star) = (\frac{\epsilon}{2}, 0)$, using only the angular velocity ω as the control of the system. The heading speed $v(t)$ cannot be controlled, but we suppose that it is known at all times. (For details on stability concepts and methods, see [7], [16].)

3.2. Motion Control under Incomplete State Information

When reconstruction of the state (y, θ) from the panoramic camera data is possible, a path-following control scheme, similar to the one developed in [10], [11], can be applied to the system ([4]).

In the case that reconstruction of the state (y, θ) from the panoramic camera data is not desirable, a motion control scheme based on the scaled difference of inverse depths, extracted directly from the optical flow corresponding to the panoramic image sequence, is possible. Two cases, however, need to be distinguished and treated differently, namely the case where the heading speed v is strictly positive or negative at all times, and the case where it is allowed to become zero.

In the case that v is time–varying, but strictly positive $(v(t) > 0, \forall t \geq 0)$, the angular velocity control $\omega_1 = -k_1\ \mathcal{L}_1^{1,2}$, with positive gain k_1 and with $\mathcal{L}_1^{1,2}$ given by 4, can be shown to locally asymptotically stabilize the system 5 to $(y_\star,\ \theta_\star)$. An input scaling procedure [11] can be used to reduce the linearization of the closed–loop system around the desired equilibrium to a linear time–invariant system.

Proposition 1 $(v(t) > 0)$

Let the heading speed v of the unicycle 1 be time–varying and assume that it is strictly positive at all times, piecewise continuous and bounded. Let d_1 and d_2 be the distances specified in the previous section. The angular velocity

$$\omega_1 = -k_1\ \mathcal{L}_1^{1,2} = -k_1\ v\ f\sin\phi\ \left(\frac{1}{d_1} - \frac{1}{d_2}\right)\ , \tag{6}$$

with gain $k_1 > 0$, stabilizes locally asymptotically the subsystem 5 of the unicycle kinematics to the equilibrium $(y_\star,\ \theta_\star) = (\frac{\epsilon}{2},\ 0)$.

Proof

The linearization of the closed–loop system around $(y_\star,\ \theta_\star)$ is

$$\dot{z} = A_1(v)\ z \stackrel{\text{def}}{=} \begin{pmatrix} 0 & v \\ -k_1 v\alpha_1 & -k_1 v\alpha_2 \end{pmatrix} z\ , \tag{7}$$

where $z \stackrel{\text{def}}{=} (z_2, z_3) \stackrel{\text{def}}{=} (y - y_\star,\ \ \theta - \theta_\star)$, $\alpha_1 \stackrel{\text{def}}{=} 8f\frac{\sin^2\phi}{\epsilon^2} > 0$ and $\alpha_2 \stackrel{\text{def}}{=} 4f\frac{\sin\phi}{\epsilon^2}(\epsilon\cos\phi + 2\delta\sin\phi) > 0$.

In 7, we can replace differentiation with respect to time t by differentiation with respect to the variable s defined by $\dot{s} \stackrel{\text{def}}{=} \frac{ds}{dt} = |v(t)|$. Since v is piecewise continuous, bounded and positive at all times, s is strictly monotonic. Differentiating z with respect to s, we get from 7:

$$\frac{dz}{ds} = A_2\ z \stackrel{\text{def}}{=} \begin{pmatrix} 0 & 1 \\ -k_1\alpha_1 & -k_1\alpha_2 \end{pmatrix} z\ , \tag{8}$$

The time–varying linear system 7 is now transformed into a time–invariant one, whose stability can be established by e.g. the Routh–Hurwitz test.

Therefore, from Lyapunov's indirect method, the nonlinear closed–loop system is asymptotically stable around $(y_\star,\ \theta_\star)$.

∎

Analysis of the second–order time–invariant linear system 8 shows that critical damping is achieved for $k_1 = \frac{4\alpha_1}{\alpha_2^2}$. This can be used as a guideline in selecting the gain of the control ω_1.

In the case that v is strictly negative, and even if it is constant, controlling the system 5 by ω_1 above, will lead to instability. The linearization of the closed–loop system can be shown to possess eigenvalues with positive real part. Therefore, a different control law is required.

Indeed, in the case that v is time–varying, but strictly negative $(v(t) < 0, \forall t \geq 0)$, the angular velocity control

$$\omega_2 = -k_2\ \mathcal{L}_1^{3,4} = k_2\ v\ f\sin\phi\ \left(\frac{1}{d_3} - \frac{1}{d_4}\right)\ , \tag{9}$$

with positive gain k_2, can be shown to locally asymptotically stabilize the system 5 to $(y_\star,\ \theta_\star)$, provided that $\epsilon \cos\phi - 2\delta \sin\phi > 0$. The proof is similar to that of Proposition 1 and is not repeated here. If ω_2 above is applied to the system when v is strictly positive, the system, again, becomes unstable.

Up to this point, we considered that the heading speed v is either strictly positive or strictly negative. It is of interest to extend these results to the case when v is allowed to cross zero. However, the previous input scaling procedure cannot be used, in this case, to demonstrate asymptotic stability of the subsystem 5 of the unicycle kinematics.

The control law ω that we consider when $v(t)$ is allowed to cross zero, consists in applying the angular velocity ω_1 of 6 when $v(t) \geq 0$ and switching to ω_2 of 9 when $v(t) < 0$. Choosing $k_1 = k_2 = k$, the control law ω is

$$\omega = \begin{cases} -k\ \mathcal{L}_1^{1,2}\ , & \text{if } v(t) \geq 0, \\ -k\ \mathcal{L}_1^{3,4}\ , & \text{otherwise.} \end{cases} \tag{10}$$

We first derive the linearization of the non–autonomous closed–loop system corresponding to the control 10.

Proposition 2 (Linearization under switching ω)

Let the heading speed v of the unicycle 1 be time–varying and assume that it is continuous and bounded. Let $(y,\ \theta) \in (0,\ \epsilon) \times (-\frac{\pi}{2}, \frac{\pi}{2})$. The linearization of the closed–loop system under the switching control law 10 is

$$\dot{x}(t) = A(t)\ x(t)\ , \tag{11}$$

where $A(t) \stackrel{\text{def}}{=} \begin{pmatrix} 0 & v \\ -k\alpha_1 v & -k(\alpha_2\ v + \alpha_3\ |v|) \end{pmatrix}$, *with* $\alpha_1 \stackrel{\text{def}}{=} 8f\frac{\sin^2\phi}{\epsilon^2} > 0,\ \alpha_2 \stackrel{\text{def}}{=} 8f\frac{\sin^2\phi}{\epsilon^2}\delta \geq 0,\ \alpha_3 \stackrel{\text{def}}{=} 4f\frac{\sin\phi\cos\phi}{\epsilon} > 0$. *This control law stabilizes uniformly asymptotically over $[0, \infty)$ the subsystem 5 of the unicycle kinematics to $(y_\star,\ \theta_\star)$, provided that the corresponding linearized system 11 is also uniformly asymptotically stable over $[0,\ \infty)$.*

Proof

The switching control law ω of equation 10 can be expressed as

$$\omega = -k\ \beta_1(y,\theta)\ v - k\ \beta_2(y,\theta)\ |v|\ , \tag{12}$$

with $k > 0,\ \beta_1(y,\theta) \stackrel{\text{def}}{=} \frac{f\sin^2\phi\cos\theta\left[2(y+\delta\sin\theta)-\epsilon\right]}{(\epsilon-y-\delta\sin\theta)(y+\delta\sin\theta)}$ and $\beta_2(y,\theta) \stackrel{\text{def}}{=} \frac{f\sin\phi\cos\phi\ \epsilon\ \sin\theta}{(\epsilon-y-\delta\sin\theta)(y+\delta\sin\theta)}$.

Applying the coordinate transformation $x_1 \stackrel{\text{def}}{=} y - y_\star,\ x_2 \stackrel{\text{def}}{=} \theta - \theta_\star$, the system equilibrium is moved to $x = 0$. The closed–loop system becomes

$$\dot{x} = f(t,x) \stackrel{\text{def}}{=} \begin{pmatrix} v(t)\sin x_2 \\ -k\ \beta_1(x)\ v(t) - k\ \beta_2(x)\ |v(t)| \end{pmatrix},$$

where $\beta_1(x) \stackrel{\text{def}}{=} \alpha_1\frac{(x_1+\delta\sin x_2)\cos x_2}{1-\frac{4}{\epsilon^2}(x_1+\delta\sin x_2)^2}$ and $\beta_2(x) \stackrel{\text{def}}{=} \alpha_3\frac{\sin x_2}{1-\frac{4}{\epsilon^2}(x_1+\delta\sin x_2)^2}$. Notice that $f(t,x)$ is continuously differentiable with respect to its second argument.

Define $A(t) \stackrel{\text{def}}{=} \left[\frac{\partial f}{\partial x}(t,x)\right]_{x=0}$, which has the form shown earlier and where $\alpha_1 \stackrel{\text{def}}{=} \frac{\partial\beta_1}{\partial x_1}(0),\ \alpha_2 \stackrel{\text{def}}{=} \frac{\partial\beta_1}{\partial x_2}(0),\ \alpha_3 \stackrel{\text{def}}{=} \frac{\partial\beta_2}{\partial x_2}(0)$.

The linearization of the closed–loop system is the time–varying linear system 11 for the matrix $A(t)$ defined above. Since v is bounded, $A(t)$ is also bounded.

Define $f_1(t,x) \stackrel{\text{def}}{=} f(t,x) - A(t)\ x$. It is easy to see by series expansion that $\lim_{||x||\to 0}\sup_{t\geq 0}\frac{||f_1(t,\ x)||}{||x||} = 0$. Thus, from Lyapunov's indirect method for non–autonomous systems [16], the result follows. ∎

Contrary to the case where v is strictly positive or negative, the linearized system is now time–varying and its asymptotic stability can be established only in special cases. We consider, then, the case when $v(t)$ is time–periodic. We establish that the linearization of the closed–loop system corresponding to the control 10 is uniformly asymptotically stable, provided that the periodic excitation $v(t)$ varies faster than the system's solution. In this case, the subsystem 5 is also uniformly asymptotically stable.

Proposition 3 (Periodic v)

Assume that the heading speed v is (i) time–periodic with period $T > 0$ (i.e. $v(t+T) = v(t)$), (ii) continuous, (iii) there exists a $T_1 \in [0,\ T)$ such that $|v(T_1)| > 0$ and (iv) $\int_0^T v(\sigma)d\sigma \neq 0$. Assume further that $\alpha_3 > \alpha_2$. Then, there exists an $\alpha_0 > 0$, such that the zero solution of

$$\dot{z}(t) = A(\alpha\ t)\ z(t)\ , \tag{13}$$

where $A(t)$ is the matrix defined in 11, is uniformly asymptotically stable over $[0, \infty)$, for all $\alpha > \alpha_0$.

The exponential stability of 13 follows from a classical averaging result [7], which considers the eigenvalues of the matrix $\bar{A} \stackrel{\text{def}}{=} \frac{1}{T}\int_0^T A(\sigma)d\sigma$. The Routh–Hurwitz test can be used to establish that, under the above assumptions, all eigenvalues of $\bar{A}$ have strictly negative real part. For linear systems, exponential stability is equivalent to uniform asymptotic stability and uniform asymptotic stability of the nonlinear system follows from Lyapunov's indirect method.

4. SIMULATION RESULTS

Fig. 4 shows MATLAB simulations of the system, where the heading speed of the mobile robot varies periodically with time ($v(t) = 0.1 + \sin t + \sin \frac{t}{2}$). The model parameters are $\epsilon = 10,\ f = 1,\ \delta = 0,\ \phi = \frac{\pi}{4}$. The switching control 10 with gain $k = 4$ is used to achieve stabilization of (y, θ) to the desired values $(5,\ 0)$ starting from the initial state $(4,\ 0.4)$.

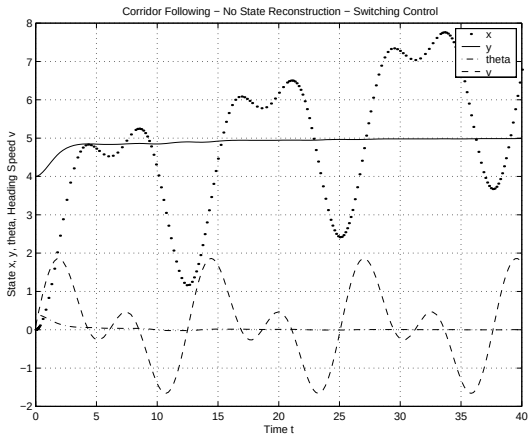

(a) State $(x,\ y,\ \theta)$ and Heading speed v

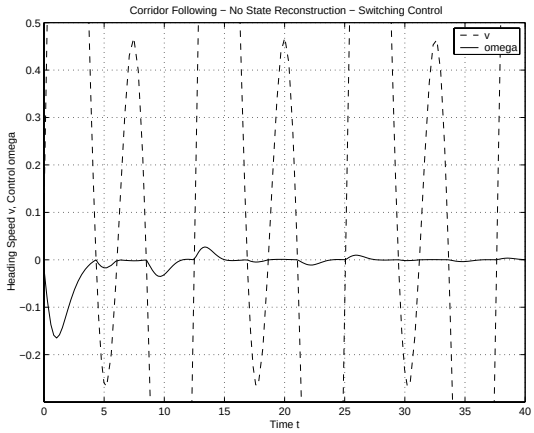

(b) Switching Control ω and Heading speed v

Fig. 4. Corridor Following: Time–Periodic $v(t)$ and Switching Control $\omega(t)$

5. CONCLUSIONS

A framework was presented for the utilization of data from panoramic images to the task of corridor following by a mobile robot. The visual servoing–type schemes derived were shown to possess the required stability properties. Further details on the stability analysis and related simulation studies can be found in [15]. Future work will focus on the experimental evaluation of these techniques, which is currently in progress.

Acknowledgments

This work was partially supported by the European Commission through project TOURBOT, contract No. IST-1999-12643, under the IST program, and by the General Secretariat for Research and Technology of the Hellenic Ministry of Development through project DRIVER, contract No. 98AMEA 18.

6. REFERENCES

[1] Argyros, A.A. and Bergholm, F., "Combining Central and Peripheral Vision for Reactive Robot Navigation", Proc. Computer Vision and Pattern Recognition Conf. (CVPR'99), Fort Collins, Colorado, USA, June 23-25, 1999.

[2] Collett, T., "Measuring Beelines to Food", *Science* **287**, 817-818, 2000.

[3] Fermüller, C. and Aloimonos, Y., "Geometry of Eye Design: Biology and Technology", Center for Autom. Res. Technical Report CAR-TR-900, Univ. of Maryland, College Park, USA, 15 pages, 1998.

[4] Gaspar, J. and Santos–Victor, J., "Visual Path Following with a Catadioptric Panoramic Camera", Proc. 7th Intl. Symposium on Intelligent Robotic Systems (SIRS'99), Coimbra, Portugal, July 1999.

[5] Hager, G.D. and Hutchinson, S., Eds., "Vision–based Control of Robotic Manipulators", Special section of *IEEE Trans. Robotics and Automation* **12**, 649-774, 1996.

[6] Horn, B.K.P., *Robot Vision*, Mc Graw–Hill, 1986.

[7] Khalil, H.K., *Nonlinear Systems*, Macmillan Publishing Co., 1992.

[8] Nayar, S.K. and Baker, S., "A Theory of Catadioptric Image Formation", Dept. of Computer Science Technical Report CUCS-015-97, Columbia Univ., USA, 30 pages, 1997.

[9] Santos–Victor, J., Sandini, G., Curotto, F. and Garibaldi, S., "Divergent Stereo in Autonomous Navigation: From Bees to Robots", *Intl. J. of Computer Vision* **14**, 159-177, 1995.

[10] Samson, C., "Path Following and Time–Varying Feedback Stabilization of a Wheeled Mobile Robot", Proc. 2nd Intl. Conf. on Automation, Robotics and Computer Vision (ICARCV'92), Singapore, 1992.

[11] Samson, C., "Control of Chained Systems: Application to Path Following and Time–Varying Point–Stabilization of Mobile Robots", *IEEE Trans. on Automatic Control* **40**, 64-77, 1995.

[12] Srinivasan, M.V., Zhang, S., Altwein, M. and Tautz, J., "Honeybee Navigation: Nature and Calibration of the 'Odometer' ", *Science* **287**, 851-853, 2000.

[13] Svoboda, T., Pajdla, T. and Hlavac, V., "Epipolar Geometry for Panoramic Cameras", Proc. 5th European Conf. on Computer Vision, pp. 218–232, LNCS 1406, Springer–Verlag, 1998.

[14] Tsakiris, D.P., Rives, P. and Samson, C., "Extending Visual Servoing Techniques to Nonholonomic Mobile Robots", in *The Confluence of Vision and Control*, Eds. Hager, G., Kriegman, D. and Morse, S., Lecture Notes in Control and Information Systems (LNCIS 237), Springer-Verlag, 1998.

[15] Tsakiris, D.P. and Argyros, A.A., "Nonholonomic Mobile Robots Equipped with Panoramic Cameras", Institute of Computer Science Technical Report ICS-TR-272, FORTH, Heraklion, Greece (to appear).

[16] Vidyasagar, M., *Nonlinear Systems Analysis*, Prentice–Hall, 1978.